CHAPTER 182

Beach Changes and Sediment Movement in the Surf Zone

Zbigniew Pruszak & Ryszard B. Zeidler [1]

Abstract

The South Baltic Sea coastal zone investigated in the years 1983–1989 belongs to multi-bar dissipative ones, with an average slope of 1.5% and sand grain size D_{50}=0.22 mm. EOF have exhibited the most common locations of bars (e_{2x}) and the most intensive bed changes (e_{3x}). Particularly conspicuous are the bed changes about the inner bar (depths about 3 m). Radioisotopic irydium glass tracers have been employed in three different subzones of the shore profile; 50–60 m from shoreline (depths h of 0.8–1.2 m), 200–250 m (h=2–3 m), and some 350-450 m (h=4–5 m), respectively.

During storms the most intensive sediment motion occurs in the second subzone, where the longshore sediment transport rate q reaches 40 to 100 kg/(m·h). Closer to shoreline (first subzone), the transport rate ranges from 15 to 40 kg/(m·h), while the smallest rate ($q \approx$ 3.5–20 kg/(m·h)) is encountered in the third subzone. Under conditions of *weak or moderate oblique waves* (e.g. mean wave period and height $\bar{T} \leq$ 3–4 s and $\bar{H} \leq$ 0.2 m in the second subzone), the longshore mode also prevailed but the ratio of longshore to cross-shore rate was lower, about 1.7:1 (13.5 versus 8 kg/(m·h)).

Core samples of tracer sand have provided estimates of the vertical extent and distribution of transport rate in the bed layer. It has been found that the thickness of the bed sublayer in which all grains move in bulk reaches $\delta \approx$ 2–5 cm during storms, versus a few grain diameters to 1.5 cm under weak and moderate waves.

1 Introduction

Most engineering activities take place in coastal areas shallower than 10 m. At the same time, these areas create most practical and scientific problems, and their exploration is still far from complete. Field measurements are usually a

[1] Assoc. Prof. & Professor; Polish Academy of Sciences' *Institute of Hydro-Engineering, IBW PAN*, 7 Kościerska, 80-953 Gdańsk

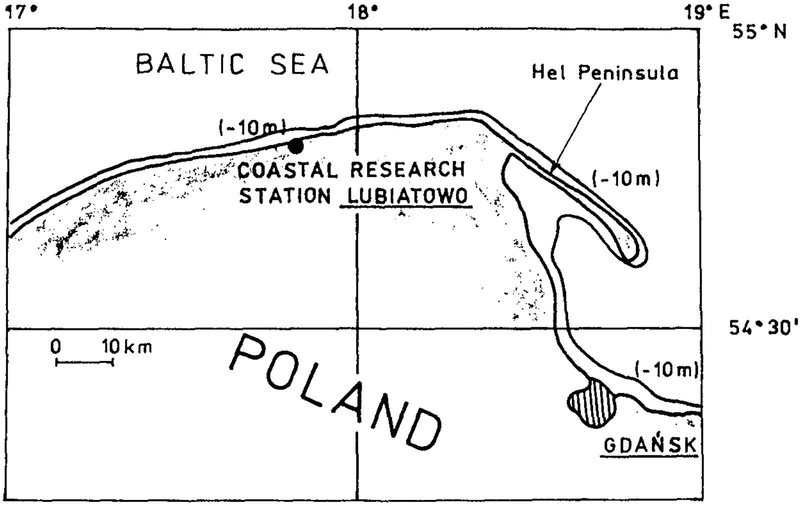

Figure 1. Location Plan of Investigation Site

prerequisite to conduct such activities. To comply with that challenge, at least in some respects, the Authors have initiated an experimental project throwing light on nearshore sediment dynamics. The paper presents results of field studies and analysis of field data relating to sediment movement and beach changes in the South Baltic Sea in the years 1983–1989.

2 Site Conditions

The investigations were conducted at *IBW PAN* Coastal Research Station at Lubiatowo, some 75 km NW of Gdańsk (Fig. 1.). The coastal zone belongs to multi-bar dissipative ones, with an average slope of 1–1.5% and sand quartz grain size D_{50}=0.22 mm and density ρ_s=2650 kg/m^3. Usual maximum storm waves have H_s=3.5–4.0 m and T_s=7–8 s at the seaward boundary of the surf zone ($h \approx 7$ m), primarily from N–NW sector.

Routine measurements of topographic features have been conducted since 1983 on a 2.7-km beach and nearshore zone extending some 800 m from shoreline. The beach profiles have been arranged every 100 m. The systematic measurements have permitted an insight into the variability of coastal features in space and time. By the use of empirical orthogonal functions (EOF) we identified the areas of most intensive dynamics, and tracer studies were carried out in such areas of pronounced bed changes (I, II and III in Figure 2), clearly coupled with underwater bars.

Radioisotopic irydium glass tracers have been employed to track the sediment movement in the three different areas of shore profile. The ^{192}Ir isotope of 74.4-day half-time had the grain diameter D=0.015–0.025 mm and density of 2668 kg/m^3, thanks to its composition (48% SiO_2, 17% Al_2O_3, 6% MgO, 5% SiO_2, 5% TiO_2, 5% K_2O and 0.25% IrO_2), thus close to natural sand.

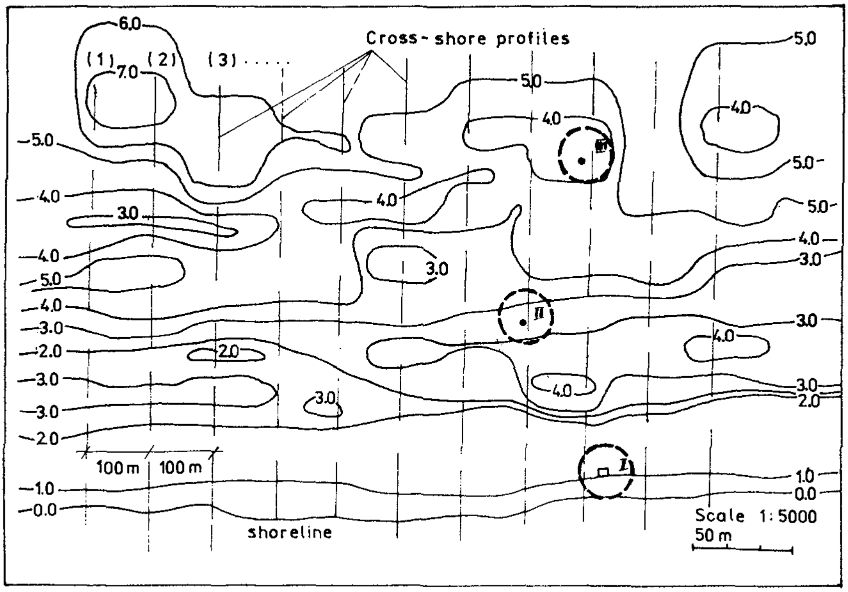

Figure 2. Bed Topography at *IBW PAN* Coastal Research Station at Lubiatowo

The movement of the tracer sand was tracked automatically, if within a special 10×10 m steel framework (referred to as 'Spider'), or from boat if far away from shoreline. The quantity of the tracer used was 100 g (area I) up to 1 kg (area II). Calibrated scintillation probes were employed to record the concentration of sand.

Measured simultaneously with changing bed topography and sand concentration were parameters of the controlling dynamics, i.e. wind, waves and currents. At least two series of bed topography measurements (beginning and end of tracer test) were executed. Wind was measured at an altitude of 5 m above MSL. Waves were recorded at a few locations along the shore profile. A waverider was deployed on a depth of 7 m, and resistance-type wave probes were installed on shallower measuring posts. Electromagnetic current meters (Interocean and Colnbrook) were placed at a few spots, primarily the stationary framework ('Spider'). Examples are shown in Figure 3.

Even a casual glance at the measured hydrometeorologic data shows a considerable nonstationarity of the factors controlling the sediment movement. Periods of intensive dynamics are preceded and followed by 'dormant' or 'stagnant' waves and currents, thus sediment transport as well. Since we have been unable to log sediment and bed characteristics at every single instant, we have focused attention on average hydrodynamical factors for some typical situations labelled 'storms' (case A) and 'medium sea' (case B). An arbitrary definition has been adopted in which 'storm waves' have $H_s \geq 0.6$–0.7 m on depths $h \approx 2$–3 m.

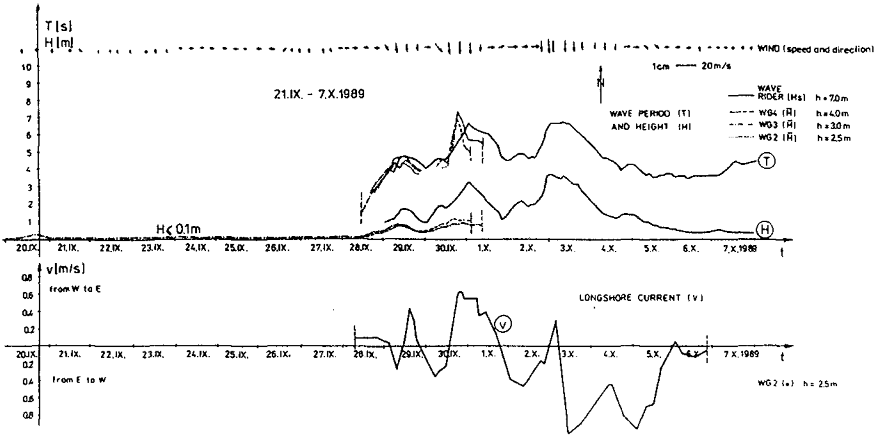

Figure 3. Examples of Measured Time Series of Wind, Waves and Currents

3 Results

3.1 Nearshore Bed Changes

Shore profile changes can be employed for reliable description of sediment movement. The profile can be presented as a sum of a certain mean component of Dean type, $y = Ax^{2/3}$, and disturbances coupled with bars, shoals, troughs etc (cf. Pruszak 1992). Such a decomposition permits identification of locations with intensive changes in bed and sediment features, judged from the variation of the disturbances (Fig. 4).

Empirical orthogonal functions prove to be an effective tool in analysis of coastal processes. The first three one-dimensional eigenfunctions $e_1(1)$, $e_2(x)$ and $e_3(x)$ have exhibited the areas where the bed phenomena were most active. These areas (I, II and III) are tightly correlated with underwater bars — as seen from $e_2(x)$ — and substantial sediment transport, coupled with concpicuous erosion and accretion, displayed in local extrema of $e_3(x)$. Major bed changes in our study area occur on water depths up to 5–6 m, while seasonal changes are encountered on slightly deeper water (6–8 m).

The results depicted in Figure 5 are typical of all distributions obtained within our study. Therefore it has been interesting to examine the locations of high dynamics by other tools. Accordingly, we have harnessed radioisotope sand tracers to shed more light on sediment dynamics.

3.2 Sediment Movement

Radioisotopic irydium glass tracers have been employed to track the sediment movement in three different subzones of the shore profile. The first one(Area I)

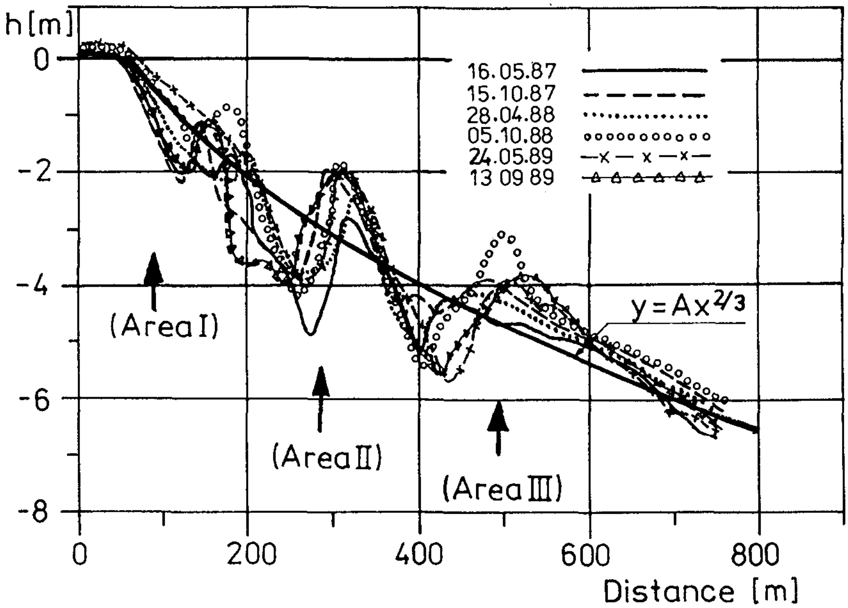

Figure 4. Examples of Measured Shore Profiles

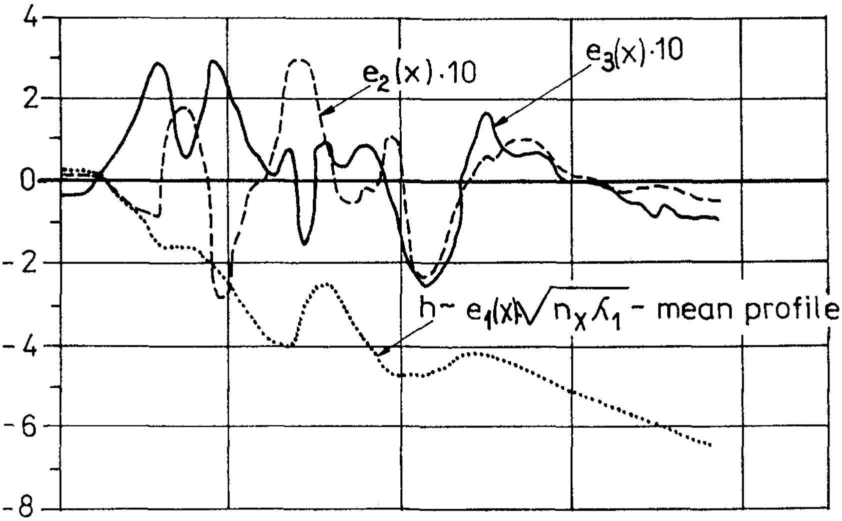

Figure 5. Eigenfunctions Computed for Lubiatowo, 1987–1989

Table 1. Sand and Water Velocities

Wave Conditions	Area (Fig. 2)	Bedload Thickness δ	Surf. Vel. $\bar{v}_s^o$, cm/h	Bulk Vel. $\bar{v}_s$, cm/h	Longsh. $\bar{v}$, cm/s
(A) 'Storm'	I	a few grain	120–150	≈50	≈40
$\bar{H} > 0.4$ m	II	dia (surface)	250–300	100–150	≈50
h=2–3 m	III	to 2–5 cm	80	≈15	–
(B) 'Med. Sea'	I	under storm	90–100	25–30	10–15
$\bar{H} \approx 0.2$–0.3 m	II	conditions	100–120	30–40	≈20
h=2–3 m	III		–	2–10	–

was spaced 50–60 m from shoreline (depths h of 0.8–1.2 m), between the steady inner bar and the ephemeral bar. Area II occurred 200–250 m from shoreline (h=2–3 m), at the outer bar, most conspicuous and lasting. Area III was most distant (some 350-450 m and h=4–5 m), encompassing the outermost bar, which delimits the seaward boundary of the surf zone.

3.2.1 *Tracer Advection Velocity*

Our measurements have confirmed that sediment transport usually occurs in two layers having different thicknesses and very different speeds. In situations with intensive waves (storms), slower motion some centimetres below static bed line is accompanied by much faster movement on the bed surface, measured in a few grain diameters (Fig. 6). Let alone for their position and weaker interlocking, the surficial grains are much more mobile, and their average speed is two or more times higher than its counterpart in the lower layer. As a result of such a double-layer transport, the tracer plume is smeared, the grains at the surface leading before slower cores some centimetres deeper in bed. An example illustrating this phenomenon in Area II is presented in Figure 7. Under lower waves ('medium sea'), the sediment movement is confined to the surface layer. The chief quantities measured in the three areas, including sand speed, are summarized in Table 1.

The sediment grain speeds have been computed for the effective duration of wave action, i.e. that above the incipient transport threshold. From the computed data one can see that sand speed $\bar{v}_s$ is 1000 times smaller than the water velocity $\bar{v}$, that is one order of magnitude less than postulated by Kraus et al. (1982) and Drapeau et al. (1990) for oceanic coast. It should be noted that our figures have been obtained in numerous experiments executed in various years. The difference can be attributed to dissimilarities in wave and tide conditions (the Baltic Sea is known as nontidal), number of underwater bars, wave breaking etc. First and foremost, however, the duration of effeetive driving forces was defined differently. The values given in Table 1 characterize mean conditions of a certain category ('storm' or 'medium sea'), averaged over lapses of time with waves above the threshold corresponding to the incipient velocity of water, estimated as 8–10 cm/s by Pruszak & Zeidler (1988).

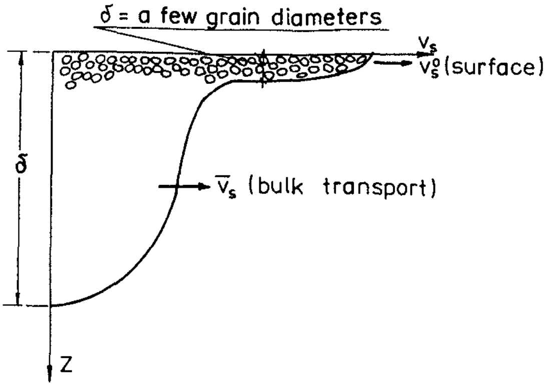

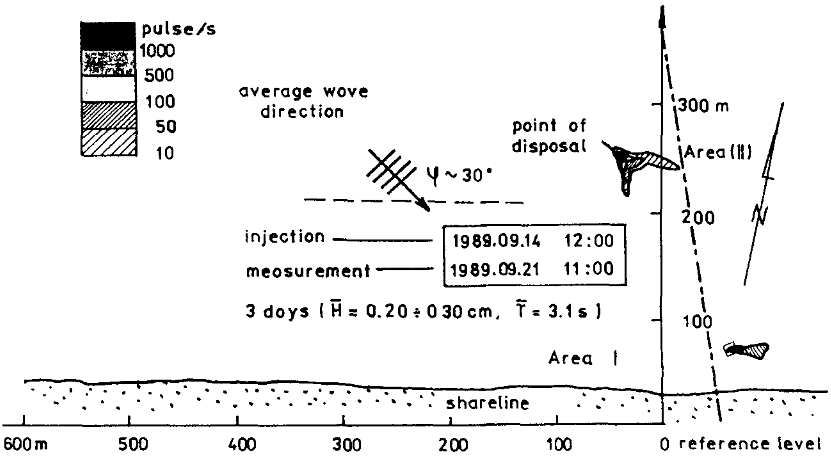

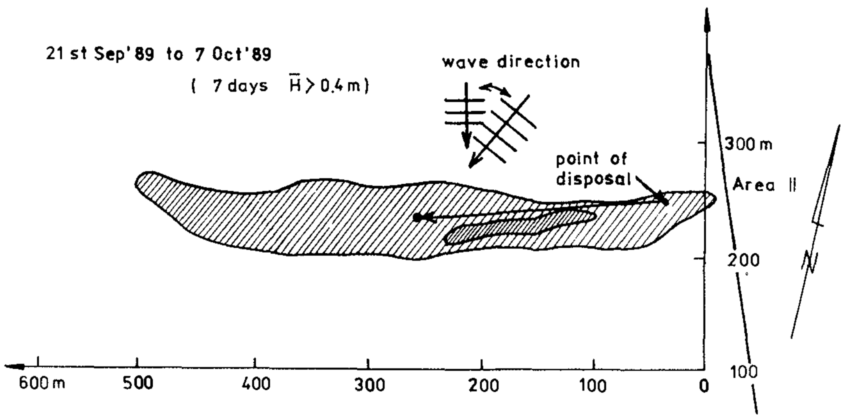

Figure 6. Schematic Sand Advection (top)
Figure 7. Distribution of Radioactive Sand Tracer fom 14th to 21st September 1989 (center) and from 21st September to 7th October 1989 (bottom).

3.2.2 *Mixing Depth*

The thickness of the bedload layer δ, in which all grains are assumed to move, has been found to vary from a few grain diameters to 2 cm under 'medium sea' conditions and 5 cm during storms. Since sand cores were cut out for analysis in layers 2 cm thick, it has appeared impossible to make finer distinctions.

Analysis of the measured data shows that sediment usually moves in a relatively thin layer (below 2 cm) if due to 'medium sea'; that thickness might be even smaller in view of the accuracy of the measurements. On the other hand, the thickness might increase in view of the intersecting paths of grains travelling in different directions and at different speed. This is particularly true for Area I, where meandering of longshore current brings about clear diversification of sediment movement. Further away from shoreline, the thickness δ is much greater, from several to a few tens of centimetres, respectively for 'medium sea' and 'storm' (Fig. 8).

Upon comparison with Kraus et al. (1982) and Drapeau et al. (1990), illustrated in Figure 9, the agreement is visible with the former, thus supporting the empirical correlation

$$\delta = 0.027 H_b \tag{1}$$

3.2.3 *Sediment Transport Rate*

Most experiments took place upon oblique wave incidence. During storms longshore current prevails, while under case B conditions the longshore and cross-shore modes are equally important. For instance, in case B Area II, the cross-shore to longshore sediment transport rate can be estimated at 1:1.7, in absolute terms roughly 8:13.5 kg/(m·h). Incidentally, the cross-shore transport in case B situations is usually onshore (Fig. 5).

The sediment transport rate is computed from the formula

$$q_i = (\rho_s - \rho)\bar{v}_s\delta \tag{2}$$

in which

q_i = transport rate in Areas I, II and III (i=1, 2, 3),
δ = thickness of sediment motion layer,
$\bar{v}_s$ = mean sediment speed in bed layer.

The ranges of δ along the shore profile are illustrated in Figure 6.

As could be expected, the highest transport rate takes place in Area II. During storms, the longshore rate reaches q=3.5–20 kg/(m·h) in Area III, 40–100 kg/(m·h) in Area II and 15–40 kg/(m·h) in Area I. These figures become about five times smaller at 'medium sea', when only two times greater than the cross-shore rate. The gross longshore transport rate across the shore profile stretching from shoreline 700 m off shore is given in Table 2, for various external factors.

Both $\bar{v}_s$ and δ vary in time and space in the two cases A and B.

Finally, one can put forth

$$q = q_i \Delta l_i (\Delta\rho)^{-1} \tag{3}$$

in which

Δl_i=width of area (I, II or III) measured along shore profile.

The total longshore transport rate in surf zone of width l varies from 1.95–6.0 m^3/s in storms to 0.35–1.95 m^3/s in medium sea.

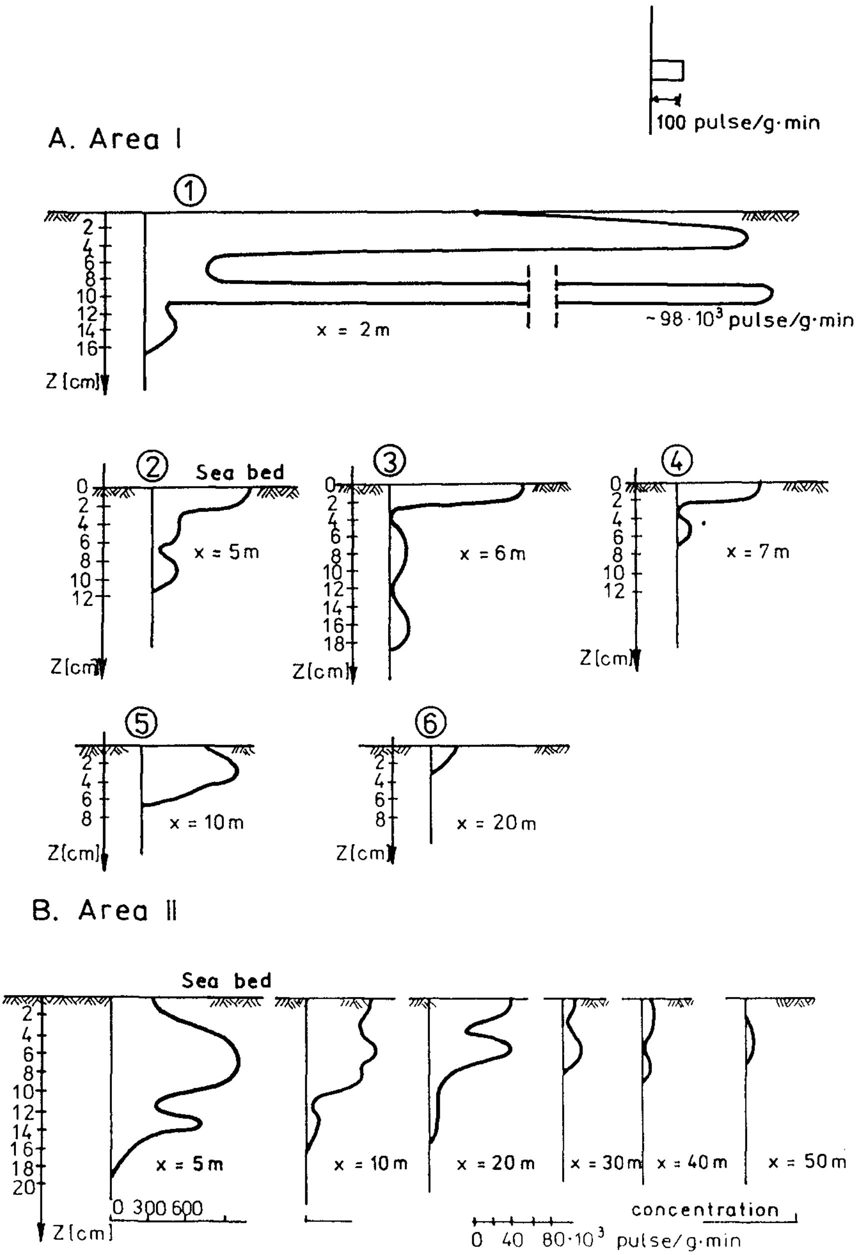

Figure 8. Vertical Distribution of Tracer Concentration

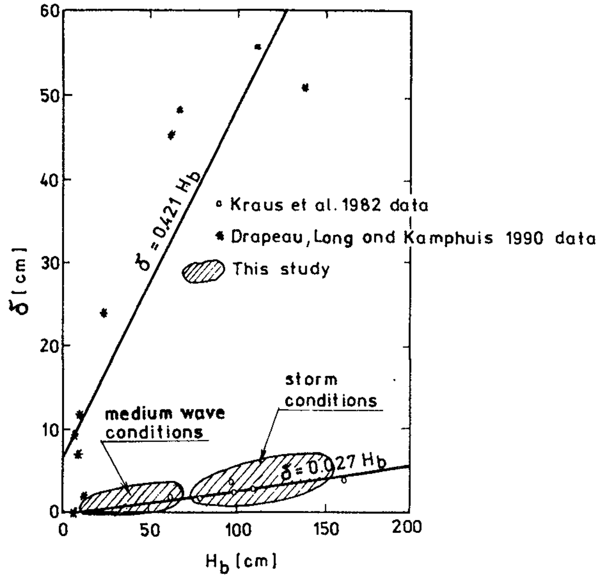

Figure 9. Depth of Mixing

Table 2. Gross Longshore Transport Rate

Case	Area (Fig. 2)	Bulk Vel. $\bar{v}_s$, cm/h	δ cm	Computed $10^{-3}q$, m^3/s	$\frac{q}{H_b^2\bar{v}} = K$	Note
(A)	I	50	2–5	1.95–6.0	0.015–0.018	(a)
	II	100-150				
	III	10–15				
(B)	I	25–30	a few	0.35–1.35	0.025–0.026	(b)
	II	30–40	grains			
	III	2–10	to 2 cm			

(a) Gross transport across l=700 m; (b) at 'medium sea' wave breaks close to point I ; $H_b \approx$ 0.5 m. During storms, H_b=0.6–1.5 m in surf zone.

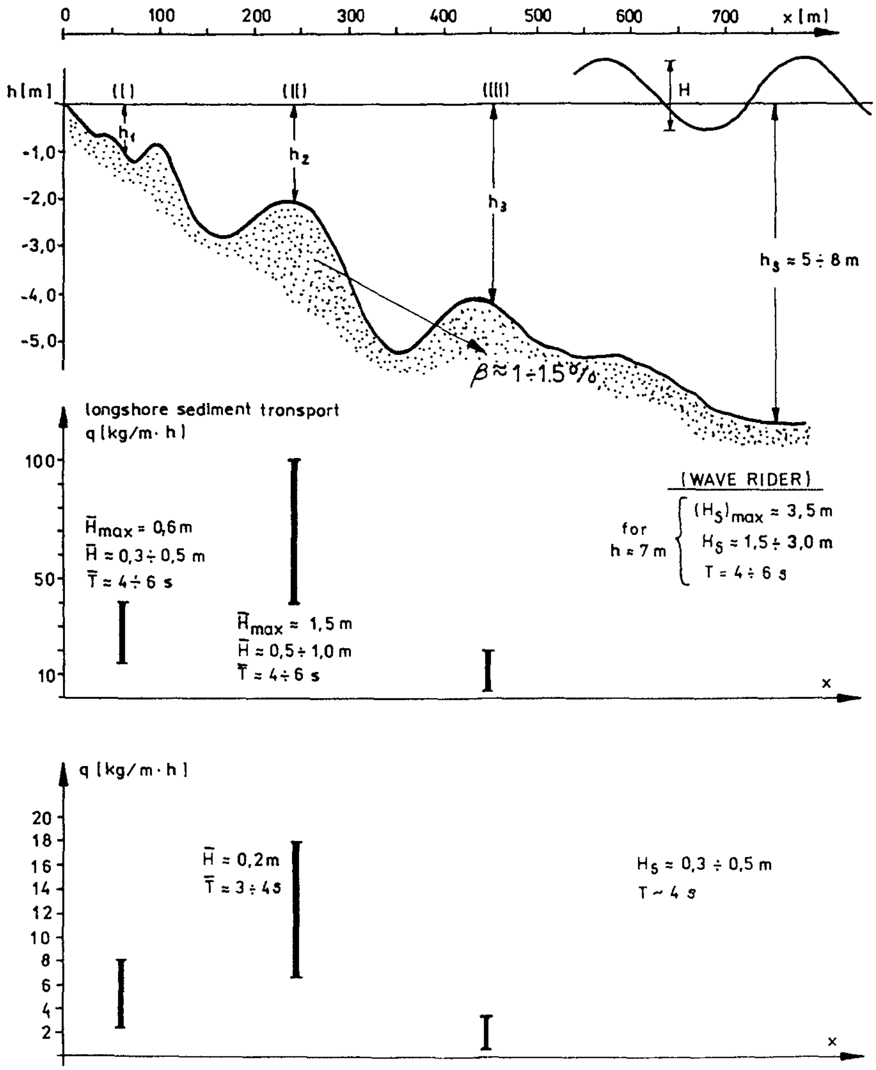

Figure 10. Sediment Transport Rate Estimates

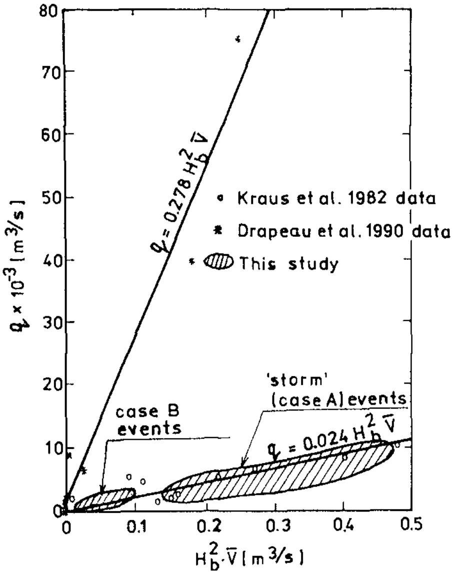

Figure 11. Volumetric Transport Rate; Global Rate, $q \sim K(H_b^2\bar{v})$

4 Comparison with Other Studies

Similar investigations have been carried out by Kraus et al. (1982) and Drapeau et al. (1990). Sediment properties (D and ρ_s), bottom slope β, wave breaking index H_b/h_b etc have been encountered by us and Kraus et al. while those of Drapeau et al. were different in some respects. The difference is thought to bring about the divergence visible in Figure 11.

Major disparity arises in the proportionality factor K put forth by Kraus et al. :

$$q = \frac{3.8 \cdot 10^{-4}}{\gamma_b \tan\beta}(H_b^2\bar{v}) = K(H_b^2\bar{v}) \quad \mathrm{m^3/s} \tag{4}$$

Kraus et al. give K=0.024 while Drapeau et al. suggest 0.278. We have established that K depends on the intensity of wave action, and becomes 0.015–0.018 in medium sea and about 0.025–0.026 under storm conditions. The dissimilarities may be attributed to various factors controlling sediment transport phenomena such as deeper penetration of wave motion during storms and the decreasing mobility of sediment grains with depth in sea bed. Energy dissipation mechanisms, different in cases A and B, are also responsible for the scatter of K.

5 Discussion and Concluding Remarks

Aside from the grain speed v_s, the thickness of bedload layer δ is difficult to measure. The magnitude $\delta \approx$ 10–60 cm given by Drapeau et al. (1982) seems overestimated. If one defines δ as the thickness of all n grain diameters in motion, then δ varies from a few D_{50} to 5 cm, depending on the intensity of wave motion.

Another problem can be seen in the identity of the movements of native sediment and tracer sand. It appears that the identity is complete over short spans of time (minutes or hours at most), whereupon the tracer speed can be deemed equivalent to the instantaneous sand speed. In longer time scales (days and weeks), the average velocities are usually smaller, roughly by one order of magnitude in our experiments. This is due to the random nature of grain motion.

The maximum sediment transport rate occurs in the active zones exhibited by EOF, i.e. usual wave breaking areas. Under storm waves, the longshore sediment transport rate grows locally up to 100 kg/(m·h), about five times more than its 'medium sea' counterpart. The gross transport rate across the entire shore profile, averaged over days, approaches 4 m^3/s during storms or 0.85 m^3/s in medium sea. These quantities refer to average conditions of mild slope (1–2%), multiple wave breaking, and medium sand (D_{50}=0.22 mm, ρ_s=2650 kg/m^3). Since such figures are quite common throughout the world, they can be suggested as general rough estimates for similar environments and time scales of days.

The coefficient of proportionality $K = \frac{q}{H_b^2 \bar{v}}$ has been found to vary from 0.025–0.026 in case B events to 0.015–0.018 in case A, thus in the range outlined by Kraus et al. (1982). Hence our field findings agree well with the earlier data by Kraus et al. (1982) but are in disagreement with the results published by Drapeau et al. (1990), inter alia their method of computing the total sediment transport rate. It is hoped that our results can modify and improve the engineering estimates of sediment transport.

Acknowledgements

The research reported on herein has been sponsored by the Polish Academy of Sciences under CPBP 02.12 and other PAN/KBN programmes, which is gratefully acknowledged. The first author expresses his gratitude to the *Stefan Batory Foundation* who granted him the *Soros* scholarship and hereby sponsored his travel to and accomodation in Venice.

References

Drapeau G., B.Long & J.W.Kamphuis (1990). Evaluation of radioactive sand tracers to measure longshore sediment transport rates. *Proceed. 22nd ICCE*, Delft, ASCE.

Krauss N.C., M.Isobe, H.Igarashi, T.O.Sasaki & K.Horikawa (1982). Field experiments on longshore sand transport in the surf zone. *Proceed. 18th ICCE*, Cape Town, ASCE.

Pruszak Z. (1992). The analysis of beach profile changes using Dean's method and empirical orthogonal functions. *Journal for Coastal, Harbour and Offshore Engineers* (in press).

Pruszak Z. & R.B.Zeidler (1988). Estimates of cross-shore bedload and bed changes. *Proceed. 21st ICCE*, Malaga, ASCE.